DEVELOPMENT OF FLUID DYNAMIC SIMULATION IN THE LADLE WITH SUBMERGED LANCE INJECTION*

Daniela Barçante Perasoli [1]
Alice Silva Gonçalves [2]
Cecilia Laia da Silva [2]
Carlos Berlini Filho [3]
Carlos Antônio da Silva [4]
Johne Jesus Mol Peixoto [5]

Abstract

For the development of the computational fluid dynamic (CFD) simulation of the ladle desulphurization process with reagent injection through a submerged lance, the calibration of interphase forces is essential to obtain a reliable prediction, which allows the distribution of gas and reactant particles throughout the domain to be known. In this work, using numerical simulations via CFX, the effect of lift, and turbulent dispersion forces in a 1:7 scale physical model of a 245ton industrial ladle was investigated. The distribution of gas predicted via CFD was assessed and validated with physical modeling results. The best combination of interphase forces was found by taking in account a virtual mass coefficient of 0.3, the turbulent dispersion force and a lift coefficient of 0.5. Mixing time was well predicted by the CFD simulations. The gas flow showed a great influence on the mixing time and off-centering the lance also reduced the mixing time.

Keywords: Hot Metal Desulfurization; Hot metal ladle; Submerged lance; CFD Simulations.

1 *Metallurgical Engineer, Master Student, REDEMAT, Federal University of Ouro Preto, Ouro Preto, Minas Gerais, Brazill.*
2 *Undergraduate Student of Metallurgical Engineering, Department of Metallurgical and Materials Engineering (DEMET), UFOP, Ouro Preto, Minas Gerais, Brazil.*
3 *Metallurgical Engineer-MSc, Technical Manager, Gerdau, Ouro Branco, Minas Gerais, Brazil.*
4 *Metallurgical Engineer-PhD., Professor, DEMET, UFOP, Ouro Preto, Minas Gerais, Brazil.*
5 *Metallurgical Engineer-Dr., Professor, DEMET, UFOP, Ouro Preto, Minas Gerais, Brazil.*

1 INTRODUCTION

In the lance injection method, the reagents are carried by an inert gas, nitrogen or argon, through a ceramic lance with nozzles located at its end. The gas bubbles with the desulphurizing particles adhered to it, rise due to buoyancy forces to the surface and during the upward trajectory the particle chemically reacts with sulfur contained in the liquid metal [1].

Wang et al. [2] studied the application of wall lubrication force and virtual mass force in order to eliminate the false phenomenon of adhered gas at the submerged lance wall. The authors proved the need to apply these forces in the construction of the model, since, without the wall lubrication force, some bubbles move towards the submerged lance under the effect of the turbulent dispersion force and, finally, the bubbles rise to the top surface, slipping along the submerged lance. In the work developed by Tripathi et al. [3] a considerable adherence of the plume to the lance wall can be noticed when studying a lance with a curved tip, suggesting that these forces were not taken in consideration. Similarly, if the virtual mass force is forgotten, the penetration depth of the injected bubble is shallow and the bubbling plume results closer to the submerged lance. In addition, the virtual mass force acts as a drag force to the bubble motion and, therefore, the axial velocity of the gas decreases when the same is taken in account, implying in more transfer of momentum to the liquid and better agitation of the liquid in the ladle [2].

In another work, Wang et al. [4] evaluated the effects of geometry and position of the lance using computational simulation, considering the use of all forces: drag, turbulent dispersion, wall lubrication, virtual mass and lift. However, the evaluated criteria and applied coefficients were not mentioned. There are many works in the literature that evaluate the influence of interaction forces between the gaseous and liquid phases on the circulation rate in the RH reactor [5, 6, 7, 8], but studies referring to the desulfurization process in ladle with reagent injection through a lance are scarce.

A careful analysis of results from many mathematical simulations available in the literature show that some of them did not achieve a good representation of the gaseous plume formed by the injection through a submerged lance. In some instance the gas remains adhered to lance walls, while in others, gas penetration is apparently excessive. According to the literature [2,3,4], the gas distribution is essential to promote energy input to the liquid and effective mixing. Thus, there is still a need to explore the best combination of interaction forces and the values of the coefficients of these forces to build a mathematical simulation that describes the behavior of the gas in a physical model, and achieve good prediction of mixing time and features of the flow pattern inside the ladle with submerged lance injection.

In this work, the effect of lift forces, virtual mass and turbulent dispersion was investigated and validated using data from a physical model of a hot metal ladle stirred by injection through a submerged lance. The effect of lance decentralization and gas flow on the mixing time was also assessed.

2 DEVELOPMENT

A water model was built so that it could provide images of bubble dispersion and mixing time by the conductimetry method. Table 1 presents geometric parameters from the industrial reactor and the model built in acrylic on a 1:7 scale.

Tabel 1. Description of the characteristics of the industrial reactor and model

Parameter	Industrial	Model 1:7
Top diameter a (mm)	3996	570.9
Top diameter b (mm)	3652	521.7
Bottom diameter a (mm)	3273	467.6
Bottom diameter b (mm)	2973	424.7
Liquid height 245t (mm)	3736	533
Liquid height 200t (mm)	3119	-
Volume 245t (L)	36600	~106.7
Submergence lance (mm)	300 to 400	40

The physical model consists of an acrylic apparatus, in a 1:7 scale of a 245 ton hot metal ladle. A submerged lance was used to simulate the injection of desulfurizer into the liquid metal**.**

The model is operated on liquid dynamic similarity defined according to Equation 1 (Froude dimensionless) and Equation 2 (turbulent Reynolds).

$$\left[\frac{V^2}{gL}\right]_{model} = \left[\frac{V^2}{gL}\right]_{industrial\ reactor} \quad (1)$$

$$\left[\frac{\rho VL}{\mu}\right]_{model} = \left[\frac{\rho VL}{\mu}\right]_{industrial\ reactor} \quad (2)$$

Where: L is characteristic length; V, the characteristic velocity; μ the turbulent viscosity; $\boldsymbol{\rho}$ is the liquid density; and g, the acceleration due to gravity.

The turbulent viscosity is given by Equation 3 [9]:

$$\mu = 5.5\ x\ 10^{-3}\ \rho L\ \left(\frac{g\ Q}{D}\right)^{1/3} \quad (3)$$

Here L stands for liquid level in the ladle; D is the ladle diameter; Q is the gas flow rate; ρ is the liquid density; and g, the acceleration due to gravity(all in SI units.

2.1 Physical Model Experiments

A technique usually employed to determine the mixing time is the conductimetry method, which consists of a pulse injection of salt solution (KCl) into the reactor while the conductivity meters (conductivity sensor) positioned at the bottom and on the side walls of the ladle continuously monitor the variation in salt concentration, by measuring the variation of water conductivity. The sensors are connected to a data acquisition board linked to a computer program, where the data of each test are stored and processed, as shown in Figure 1. The tests were performed with gas flow rates of 10, 15 and 20 L/min, and two lance positions: centralized and decentralized (following the industrial scale, ~0.25 of ladle radius). A total of 10 tests were performed for each experimental condition.

The dispersion of oil droplets (soybean oil colored with blue dye) injected through the lance was simulated to represent the flow of desulphurizer in the ladle with the lance centered. To characterize the gaseous plume in the model, footage was taken using a high-resolution camera. Image analysis was performed using VirtualDub software. The images were compared with results of mathematical simulations.

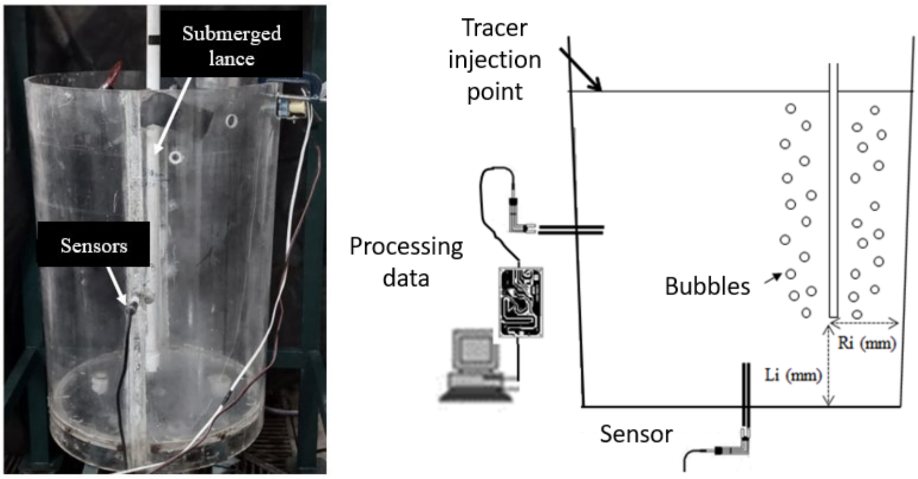

Figure 1. Photo of the acrylic model and assembly diagram for the homogenization time tests. Geometric parameters: Ri – radial position e Li – immersion depth.

2.2 Mathematical Model

The commercial software CFX 22R1(Ansys®) was used for mathematical modeling. It is based on the finite volume technique, in which the computational domain is divided into an integer number of sub-domains called elements, which maintain the same properties as the original medium. The mass conservation, momentum and turbulence equations are discretized and solved using interactive methods for each control volume. In addition, the software allows choosing turbulence models and simulating the flow in steady state or transient state. The k-ε turbulence model was used, where k represents the kinetic energy of turbulence, ε is the turbulent energy dissipation rate, coupled to the Navier-Stokes and Continuity equation.

Continuity equation (Eq. 4)

$$\frac{\partial(\alpha_q \rho_q)}{\partial t} + \nabla(\alpha_q \rho_q \vec{u}_q) = 0 \tag{4}$$

Momentum conservation equation (Eq. 5)

$$\frac{\partial(\alpha_q \rho_q \vec{\mu_q})}{\partial t} + \nabla . (\alpha_q \rho_q \vec{u}_q \vec{u}_q) = -\alpha_q \nabla p + \alpha_q \rho_q \vec{g} + \nabla . (\alpha_q \mu_{eff,q} (\nabla \vec{u}_q + (\nabla \vec{u}_q)^T)) + \vec{F_q} \tag{5}$$

* Technical contribution to the 52º Seminário de Aciaria, Fundição e Metalurgia de Não-Ferrosos, part of the ABM Week 7th edition, August 1st-3rd, 2023, São Paulo, SP, Brazil.

Symbology regarding equations 4 and 5 is as follows: subscript q represents the gas and the liquid respectively, g the gravitational acceleration, F_q the forces acting on the interface, αq is the volumetric fraction, ρq, $\overrightarrow{\mu_q}$ e μeff,q are density, viscosity and effective viscosity respectively.

The geometry was described by the Design Modeler software and the mesh was built using the Meshing Modeler software, with predominant tetrahedral elements. In the plume formation region and in the injection nozzles, a localized refinement with element size of 4mm and 1mm, respectively, was applied. The inflation tool was applied to all reactor walls, with 5 layers and the transition ratio parameter was set 0.3. The skewness parameter is used to evaluate the mesh quality. The final mesh had about 625 thousand nodes (element nodes), see Figure 2.

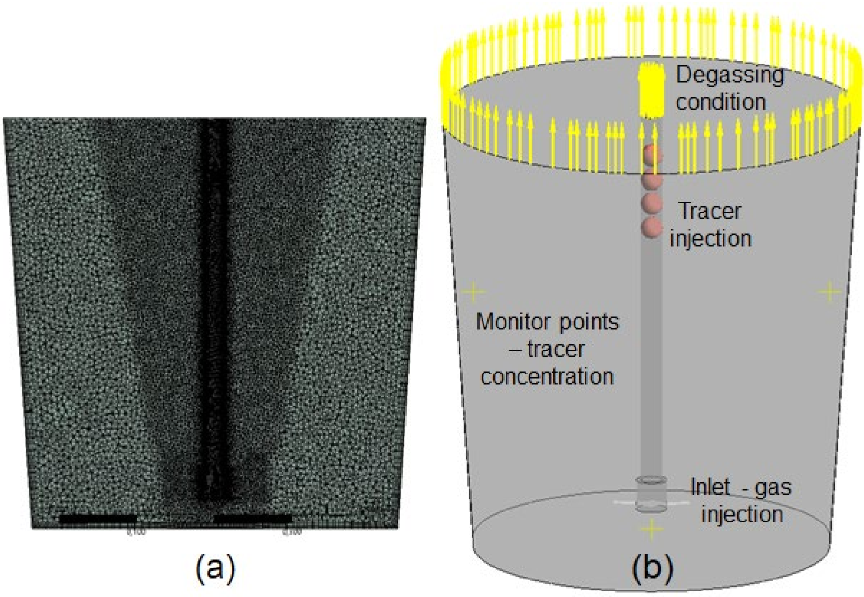

Figure 2. (a) Mesh built for the model; (b) setup configuration of boundary conditions.

2.2.1 Interfacial forces and boundary conditions

The computational simulation of two fluid phases containing a dispersed phase (gas bubbles injected by the lance) requires the use of an interphase forces model, which must find the best combination of forces to predict the gaseous plume. Existing models in CFX for such forces – drag, lift force, virtual mass force, wall lubrication force – were tested in order to obtain a combination of forces that best represented the physical model tests. The forces below are described in the Ansys tutorial [10] and in the work of Peixoto et al. [7].

Lift force: mainly caused by the existence of a velocity gradient in the liquid flow field (Eq. 6), which is perpendicular to the main flow direction, acting on the gas bubble:

$$\vec{F}_{Lift} = -C_L \rho_l \alpha_g (\vec{u}_g - \vec{u}_l) \times (\nabla \times \vec{u}_l) \qquad (6)$$

C_L is the lift coefficient, which for viscous flow, ranges from 0.01 to 0.5.

Virtual mass force: also called added mass force, the virtual mass effect (Eq. 7) can occur when a bubble accelerates relative to the liquid and is defined as follows:

$$\vec{F}_{VM} = C_{VMF}\rho_l\alpha_g\left(\frac{d_l\vec{u}_l}{\delta_t} - \frac{d_g\vec{u}_g}{\delta_t}\right) \qquad (7)$$

C_{VMF} is the virtual mass coefficient, and has a value of 0.5 for inviscid flow around an isolated sphere. In general, it depends on the shape and concentration of the bubbles and must be specified. In this work, the value C_{VMF} = 0.3 was adopted according to the results for RH degasser from Peixoto et al. [7].

Turbulent dispersion force: it can act on the bubble due to turbulence fluctuation of the liquid (Eq. 8). The model used in this work is the model based on the Favre average (or mass-weighted average) of the drag force, more indicated in situations where an appropriate value for the turbulent dispersion coefficient, C_{TD}, is known:

$$\vec{F}_{TDF} = -C_{TD}C_{cd}\frac{v_l}{\sigma_{lg}}\left(\frac{\nabla\alpha_g}{\alpha_g} - \frac{\nabla\alpha_l}{\alpha_l}\right) \qquad (8)$$

C_{cd} is the momentum transfer coefficient for the drag force; vl is liquid specific volume; σ_{tc} is the turbulent Schmidt number, usually 0.9; C_{TD} is a user multiplier coefficient. Its default value of 1.0 was considered in this work.

Symbology regarding equations 6,7 and 8 is as follows: α_i, ρ_i and u_i are, respectively, volumetric fraction, density and velocity of the liquid phase (i=l) and gas phase (i=g); g – acceleration due to gravity, μ_l – viscosity of the liquid and d_g – diameter of the gas bubble.

The existing mathematical models in CFX for drag and non-drag forces were tested in order to obtain a combination between these forces that results on the best equivalence to results from the physical model. The boundary conditions are:
• Non-slip condition (regions where the fluid has zero velocity) applied to all walls;
• Lance nozzles – inlet condition with the gas mass flow rate (kg/s) set equivalent to 10 L/min, 15 L/min or 20L/min;
• the ladle surface - as a flat region that only allows the exit of the gas and without friction with the adjacent phases (degassing condition);
The bubble diameter was assumed to be constant, being ignored their disruption and coalescence. The bubble diameter was estimated according to the expression established by Sano and Mori [11] (Eq. 9).

$$d = \left[\left(\frac{6\sigma {d_0}^2}{\rho_l}\right) + 0.0248(Q^2 d_0)^{0.867}\right]^{\frac{1}{6}} \qquad (9)$$

Where σ is the gas-liquid surface tension coefficient [Nm-1]; d_0 is the diameter of the gas outlet hole [m]; Q is the gas flow [m^{3}s-1] and ρ_l the liquid density.

Tracer dispersion was simulated using an additional variable representing the tracer, and a pulse injection (source point) for 1 s. Fluid flow results from steady state simulations were used as initial condition. It was done in transient state mode (timescale of 0.005s) and the total simulation time was 60s. Three monitor points assessed concentration of tracer at positions equivalent to the conductimeters in physical modeling.

2.3 Results and Discussion

Figure 3 shows frames of the physical model footage. The ascending plume with a higher concentration of gas can be seen around the lance and also the penetration of the gas halfway from the extremities (model walls). The transient behavior of the plume due to turbulence was noted: the plume was not symmetrical, at times there was a displacement to the right side (image at 3 s, as an example), and then the plume is displaced to the left side (image at 15 s). Tracer dispersion also stressed this behaviour. First, tracer spread on one side, until 5 s, then it spread throughout the entire ladle.

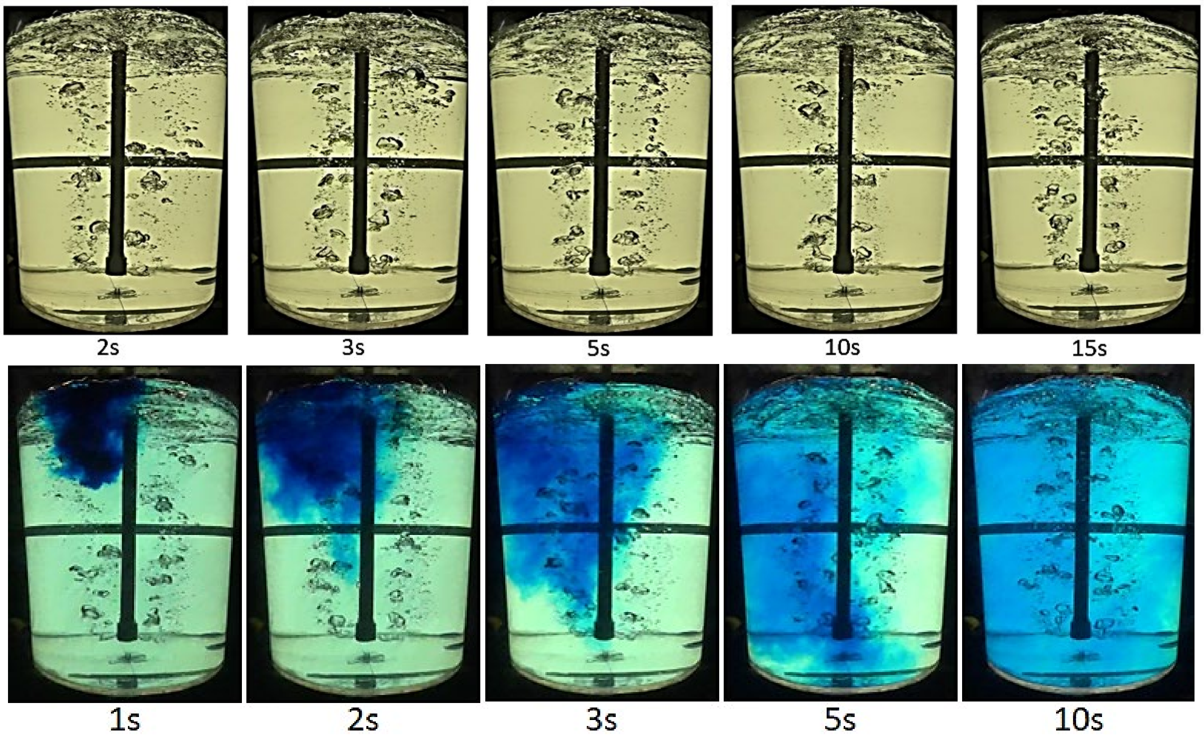

Figure 3. Characterization of the plume (a) and tracer dispersion (b) for the centralized lance, at a flow rate of 15 L/min.

Figure 4 presents images of the gaseous plume obtained by simulation for different combinations of non-drag forces. The drag force is present in all cases, due to its importance in viscous flow. The virtual mass force with coefficient (C_{VMF}) equal to 0.3 and the wall lubrication force (Frank model) were adopted, following the work developed by Peixoto et al. [7] when simulating the RH reactor. It is noticed that the incorporation of the turbulent dispersion force (Figure 4.b) alone does not allow a description of the horizontal component of gas penetration, which is smaller than the penetration observed at the physical model (Figure 3.a). The combination that best represented the behavior of the gaseous plume is described by the combinations of lift forces and turbulent dispersion (Figure 4.c). It is then possible to observe a better developed velocity profile in the transverse and longitudinal sections as a function of gas flow rate, reducing the dead zones highlighted at the bottom of the model (Figures 4.a and 5.c).

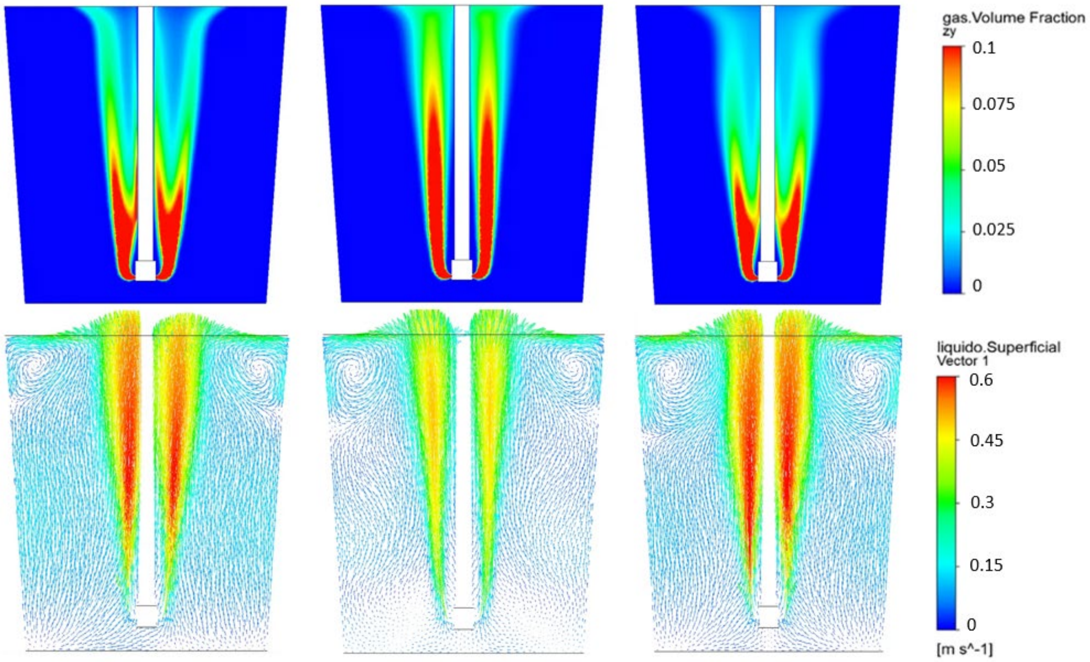

(a) Lift force (C_L= 0.5). (b) Turbulent dispersion force (C_{TD}=1) (c) Turbulent dispersion force (C_{TD}=1) and Lift force (C_L= 0.5).

Figure 4. Influence of non-drag forces on the formation of the gaseous plume and velocity field, applying drag, virtual mass (C_{VMF} = 0.3) wall lubrication forces and: (a) lift force (C_L=0.5); (b) turbulent dispersion force (C_{TD}=1); (c) C_{TD}=1 and C_L=0.5. Transversal view.

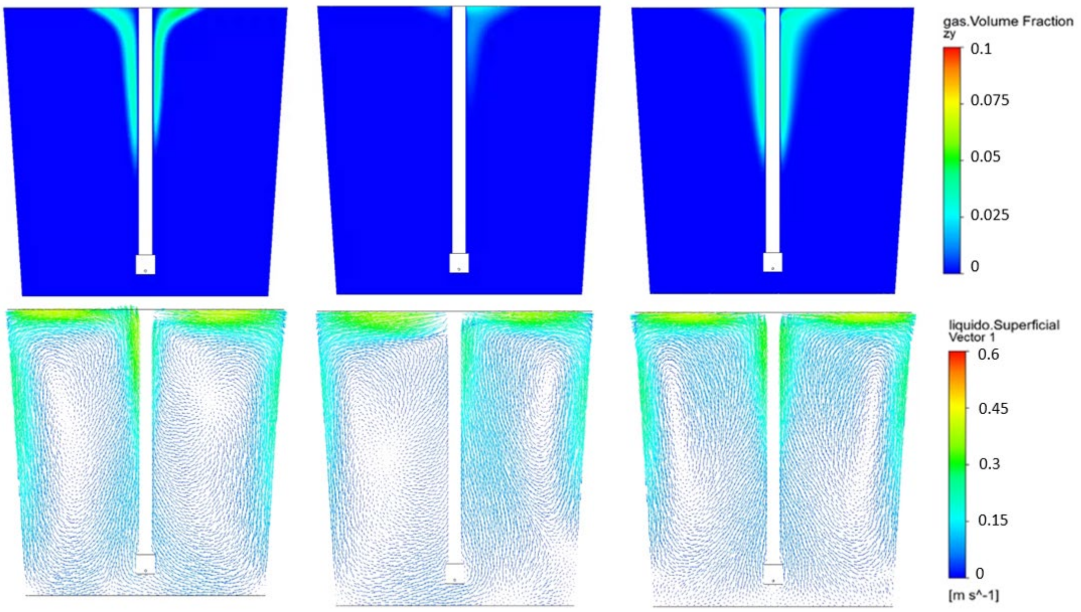

(a) Lift force (C_L= 0.5). (b) Turbulent dispersion force (C_{TD}=1) (c) Turbulent dispersion force (C_{TD}=1) and Lift force (C_L= 0.5).

Figure 5. Longitudinal view of gas plume and velocity profile for different non-drag forces: (a) C_L=0.5; (b) turbulent dispersion force (C_{TD}=1); (c) C_{TD}=1 and C_L=0.5.

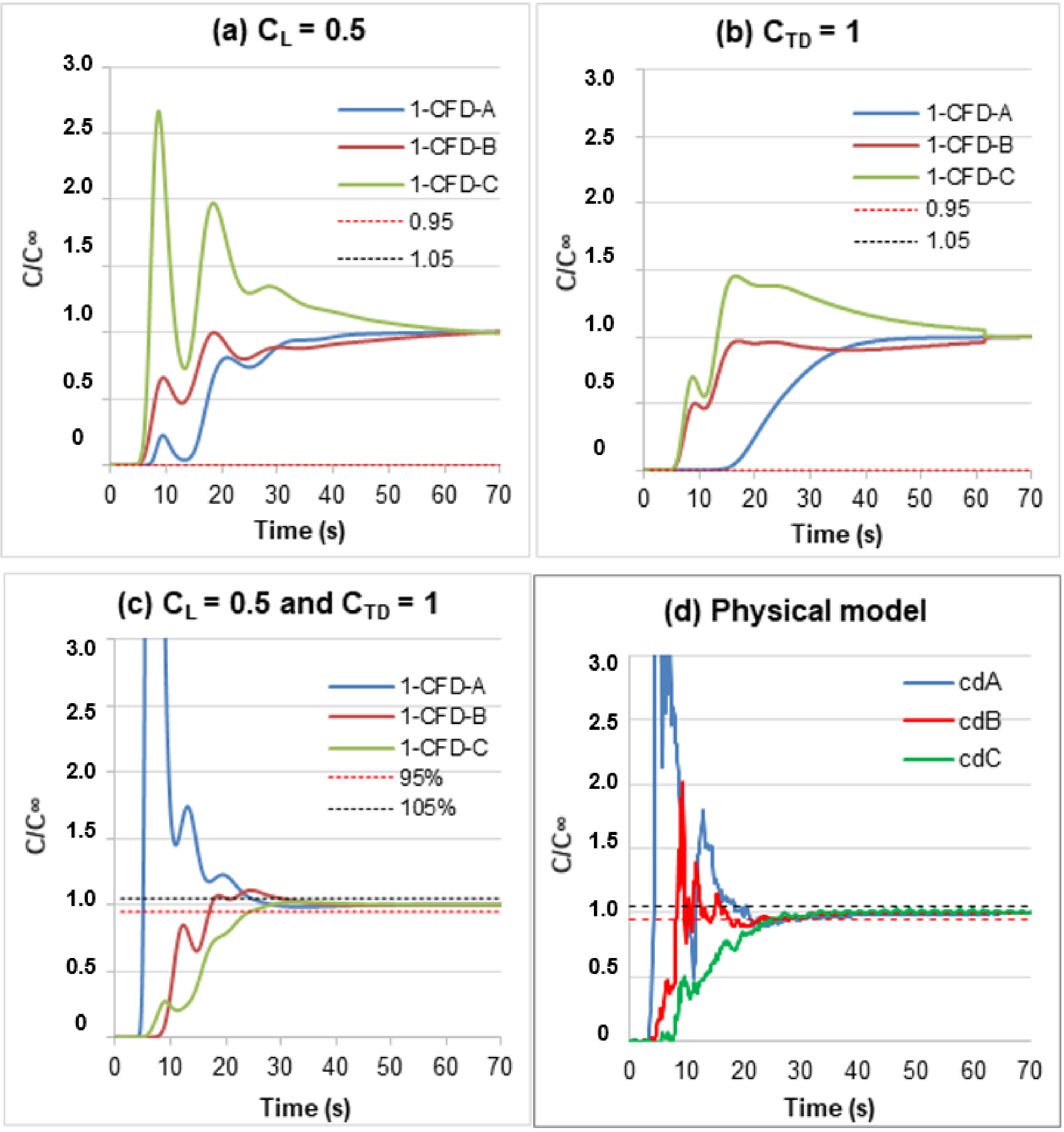

Figure 6. Normalized concentration curve for each combination of non-drag forces: (a) C_L=0.5; (b) turbulent dispersion force (C_{TD}=1); (c) C_{TD}=1 and C_L=0.5; (d) typical result from conductimetry experiments. Gas flow rate 15 L/min.

The data presented in Figure 7 report the mixing time and the respective standard deviation (physical model results) as a function of the gas flow for two lance positions. It is noticed that the mixing times from the physical model and from the computational simulation (CFD) agree very well, if one takes in account the standard deviation of the physical model. In addition, the decentralization effect of the submerged lance is beneficial to reduce the homogenization time. According to the present simulations decentering the lance would allow to reduce the gas flow to 10 L/min from 15 L/min without compromising mixing.

Comparison of the velocity profiles of centralized and decentralized lance, Figure 8, it allows one to observe the formation of zones of a larger vortex along the height of the liquid. Despite the lesser agitation at the bottom of the ladle, this larger vortex is decisive for the reduction of mixing time. This behavior was also observed by Wang et al. [4], in which the liquid velocity becomes more uniform and the mixing time and total volume of gas in the ladle gradually decrease. However, as the eccentricity increases, the velocity of the liquid near the side wall increases, which reduces the service life of the refractory. An eccentricity of 0.2 was recommended to obtain greater mixing efficiency and longer refractory life in a 1:5 scale model of a 180 ton ladle [4]. Finally, as the gas flow rate increases, the mixing time decreases, due to the larger amount of momentum transferred to the liquid.

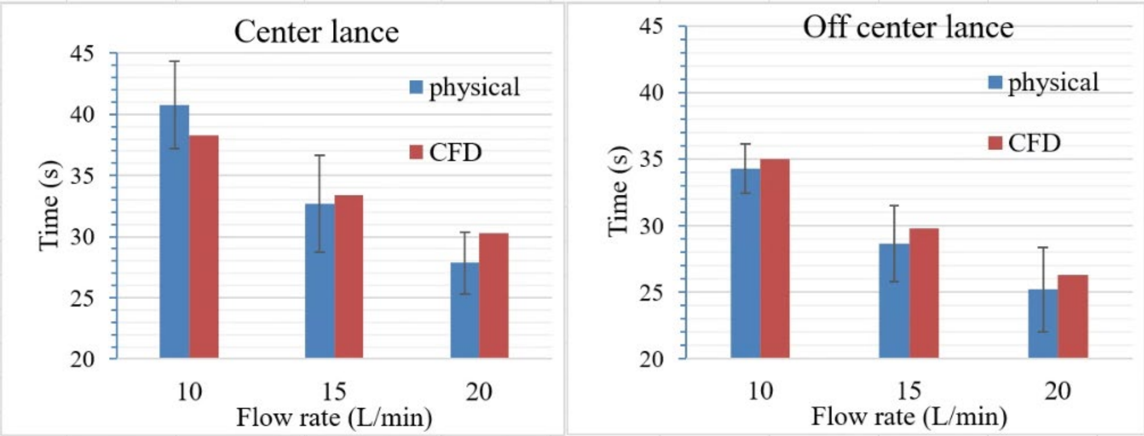

Figure 7. Comparison of mixing time for different flows and radial position of submerged lance.

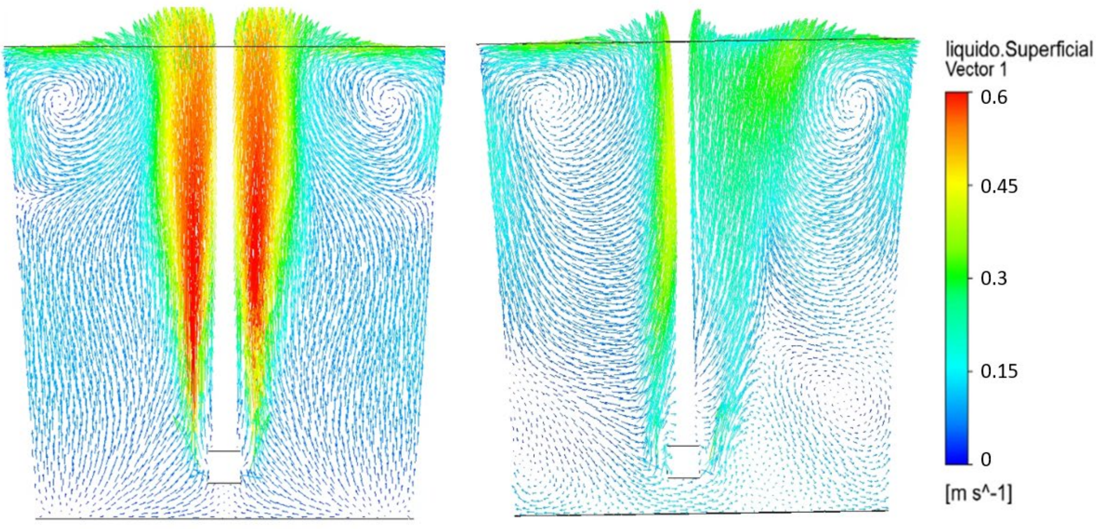

Figure 8. Comparison of the velocity profiles according to the radial position of the injection lance (flow: 15L/min and without rotation).

The behavior of the injected oil drops with the submerged lance in the centralized position was also evaluated. Figure 9 reproduces some frames of the recording in which it is possible to see that the oil drops follow an upward flow around the lance and begin to accumulate on the surface (top slag formation). Finally, an image of the physical model is compared with the computational simulation (Figure 10), suggesting that the dispersion behavior of the oil droplets was well predicted by CFD simulation.

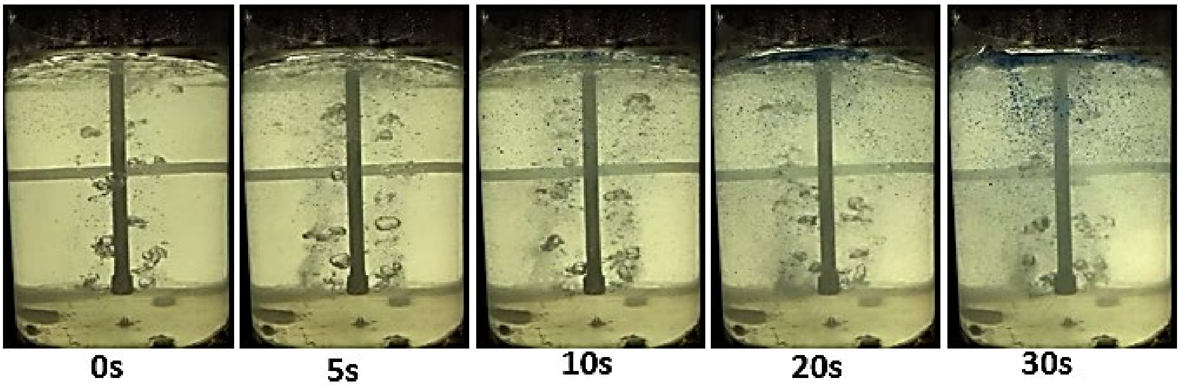

Figure 9. Dispersion behavior of oil drops in physical model for gas flow rate 5 L/min, centralized lance.

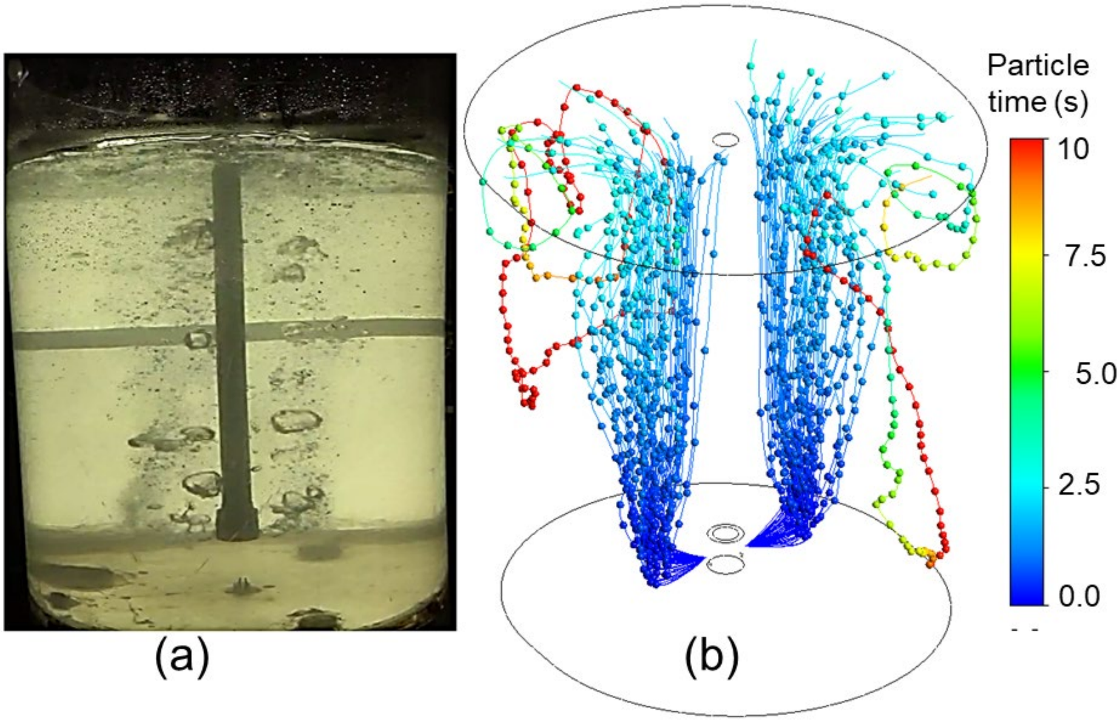

Figure 10. Dispersion behavior of oil drops in (a) physical and (b) computational modeling.

The results reinforce the expected mechanism for desulphurization via lance by injecting reagents, in which the carrier gas flow, the trajectory and residence of the bubbles in the hot metal and the fluid dynamic behavior (influenced by the radial position of the lance) are decisive for obtaining effective treatment.

3 CONCLUSIONS

The images of the gaseous plume were used to validate the CFD simulations, seeking to evaluate effects of lance position and the flow rate of carrier gas at a desulfurization process performed by deep reagent injection. The results of mathematical simulation with incorporation of non-drag forces showed that:

- In steady state simulations, the lubrication force must be used to avoid the accumulation/ adhesion of gas to the lance wall;
- The lift and turbulent dispersion forces were important to increase gas penetration in the liquid flow in the injection region (lance nozzles);

- The best combination of forces was achieved by using the virtual mass coefficient C_{VM} of 0.3, lift coefficient C_L of 0.5 and turbulent dispersion C_{TD} of 1;
- The decentralization of the lance was beneficial to reduce the mixing time, allowing a reduction in the gas flow to obtain satisfactory results.

Acknowledgements

The authors would like to thank Gerdau Usina Ouro Branco, Pyrometallurgy and Simulations Laboratory (LaPSim) at UFOP, CNPq and FAPEMIG.

REFERENCES

1 BARRON, M. A.; MEDINA, D. Y.; REYES, J. A Straightforward Mathematical Model of Hot Metal Desulphurization. Open Journal of Applied Sciences. 2020; 10, 318-327.

2 WANG, X.; ZHENG, S.; ZHU, M. Numerical simulation on gas–liquid multiphase flow in hot metal ladle with top submerged lance. Ironmaking & Steelmaking. 2019; 47, 915-924.

3 Tripathi, P.; Kumar, D. S.; Sah, R.; Sekhar, V. R. An improved lance design for hot metal de-sulphurisation. Ironmaking & Steelmaking. 2016; 44, 421-429.

4 WANG, X.; ZHENG, S.; ZHU, M. Optimization of the Structure and Injection Position of Top Submerged Lance in Hot Metal Ladle. ISIJ International. 2021; 61, 792-801.

5 Chen G, He S, Li Y, Guo Y, Wang Q. Investigation of Gas and Liquid Multiphase Flow in the Rheinsahl–Heraeus (RH) Reactor by Using the Euler–Euler Approach. JOM. 2016; 68 (8): 2138-2148.

6 Neves L. Modelagem do escoamento multifásico no desgaseificador RH e no distribuidor de lingotamento contínuo [tese de doutorado]. Belo Horizonte: UFMG; 2012.

7 PEIXOTO, J.J.M.; GABRIEL, W. V.; OLIVEIRA, T.A.S; BARONY, N.B.; SILVA, C.A.; SILVA, I.A.; SESHADRI, V. Influência das Forças de Interação Líquido/Gás na Análise Via CFD do Reator RH. In: 48º Seminário de Aciaria, Fundição e Metalurgia de Não-Ferrosos, 2017, São Paulo: Editora Blucher, v.48. p.356 – 367. http://dx.doi.org/10.5151/1982-9345-30378

8 ZHU, B.; LIU, Q.; KONG, M.; YANG, J.; LI, D. and CHATTOPADHYAY, K. Effect of Interphase Forces on Gas–Liquid Multiphase Flow in RH Degasser, Metall. Mater. Trans. B, v. 48B, p. 2620–2630, 2017.

9 Guthrie,R.I.L, Engineering in Process Metallurgy; Oxford University Press, 1992

10 ANSYS: ANSYS CFX- Theory Guide 17.1. Canonsburg: ANSYS; 2016.

11 M. Sano and K. Mori: Trans. Jpn. Inst. Met., 17 (1976), 344.